(for NAS 9-11329)

TELEVISION OBSERVATIONS OF ARTIFICIAL AURORA AND ANALYSES OF FLIGHT DATA FROM NASA PAYLOAD 12.18 NE

FINAL REPORT

NASA Contract No NAS9-11815

October 1974

GEOPHYSICAL INSTITUTE

of

UNIVERSITY OF ALASKA

FAIRBANKS, ALASKA 99701

Prepared for

NASA
Johnson Space Center
Houston, Texas

T. N. Davis
Principal Investigator

TELEVISION OBSERVATIONS OF ARTIFICIAL AURORAL AND ANALYSES OF FLIGHT DATA FROM NASA PAYLOAD 12.18 NE

1. Introduction

An accelerator nominally capable of ejecting pulses of electrons up to 6 sec in length, current to 500 ma and energy to 20 Kev was flown on a rocket at 1500 October 15, 1972. The rocket, a Strypi, was launched from the Pacific Missile Range Facility at Kauai, Hawaii. The intent was to eject electron pulses of various characteristics upwards along the magnetic field so as to produce artificial auroras in the conjugate (southern hemisphere) atmosphere and possibly to produce weaker auroras in the nearby atmosphere as a consequence of backscattered electrons. To facilitate this end, the accelerator package included a gas jet actuated attitude control system controlled by gyros. Attitude sensing also was accomplished by a two-axis fluxgate magnetometer. Also, a large foil was deployed to collect ambient electrons to neutralize the accelerator when it ejected high-energy electrons. Scientific instrumentation contained on the flight package included retarding potential analyzers (RPA), energetic electron detectors, and detectors to sense very low frequency (VLF) radio noise. Image Orthicon television systems and other optical sensors were operated in the conjugate region aboard two NC-135 jet aircraft based in Samoa. Similar devices were operated at Haleakela, Hawaii, to attempt detection of auroras caused by backscattered electrons.

This experiment was a follow-on to a similar experiment conducted in January, 1969 at Wallops Island, Virginia, wherein the accelerator was aimed downward to produce detectable artifical auroras in the atmosphere directly below the rocket. (Hess, 1965; Hess et al. 1971; Davis et al. 1971).

II. Flight Performance and Brief Summary of Initial Results

After launch the Strypi rocket followed a near-nominal trajectory for 150 sec at the end of which time the payload was ejected from the rocket. At 160 sec the payload underwent a violent altitude maneuver suggesting that it might have been bumped by the rocket vehicle. Failure of the VLF sensor system occurred at this time. It now appears that the payload underwent unscheduled attitude maneuvers during the remainder of the flight.

A programmer commanded the accelerator to fire a 44-pulse sequence of pulses of various lengths, currents and voltages over an interval of 95 sec as shown in Fig. 1. The pulse sequence was actuated at the nominal time (T+180 sec). This first sequence has been labeled the A sequence; it was followed by B, C, D and part of the E sequence, the latter being terminated on re-entry to the dense atmosphere. It was expected that artificial auroras would be detected in the conjugate hemisphere throughout the programmed pulse sequences. However no auroras were detected until one caused by pulse B44 was recorded by television systems on one of the aircraft in the conjugate hemisphere. No other artificial auroras were detected, however during some of the pulses the TV systems were not properly directed to detect any auroras that might have been produced; see Fig. 2.

III. Experiment Participants and Responsibilities

A. Participants other than the University of Alaska

1. NOAA - Dr. Wilmot Hess of NOAA conceived the experiment and played a major role in its organization and conduct. He also pursued theoretical calculations to help interpret the results.

2. NASA - Mr. Mickey Trichel, Johnson Space Center, has been the key organizer to bring the various participants together, to oversee the construction of the electron accelerator and to act as contract monitor over those participating groups funded by NASA. Mr. Russell Groves of Goddard Space Flight Center oversaw the design and assembly of the accelerator payload, preflight testing and management during flight. Dr. E. R. Maier of Goddard Space Flight Center provided retarding potential analyzers for the flight package.
3. Ion Physics - Mr. Robert Harrison of Ion Physics, Corp. managed the construction of the electron accelerator and participated in its flight.
4. University of Minnesota - Dr. D. G. Cartwright of the University of Minnesota provided the VLF sensors on the flight package.
5. Los Alamos Scientific Laboratory and Sandia Laboratory - The launch of the accelerator was conducted as part of Operation Picaposte, a rocket launching expedition involving mainly shaped charge barium experiments performed at Poker Flat, Alaska and Kauai, Hawaii. Both LASL and Sandia were major participants in this operation and made substantial contribution to the accelerator experiment in many ways. In addition to numerous other supporting functions these AEC-sponsored organizations provided the Strypi rocket and its launching two NC-135 aircraft observing platforms and operation of several scientific instruments, mainly optical, for observation of experiment results.

B. University of Alaska Participation

Our group at the Geophysical Institute of the University of Alaska was involved in the experiment in several ways:

1. There was a general involvement in experiment planning, including computation of expected locations of artificial auroras and flight plans for the observing aircraft. In this effort we employed information on magnetic field line topology gained from our earlier field line tracing experiments using the shaped charge barium technique. Dr. E. M. Wescott and Mr. H. Stenbaek-Nielsen performed much of this work.
2. A package containing three channeltron detectors to measure energetic electrons at 6Kev and 12Kev was designed by Dr. A. D. Johnstone. It was flown as the accelerator payload under the direction of Dr. J. Boyd. (Both Johnstone and Boyd were graduate students at the time).
3. The primary means of detecting and locating artificial auroras was the use of image orthicon televisions provided by us under the direction of Dr. T. N. Davis. These systems were deployed on the two aircraft and at Haleakala, Hawaii. Personnel involved were Dr. E. M. Wescott, Mr. T. J. Hallinan, Mr. L. R. Sweet, Mr. G. F. Meltvedt and Mr. R. F. Beach.
4. Our group has performed essentially all analysis of the television and other supporting data acquired on the aircraft. We also have done the bulk of the analysis of the flight data because NASA curtailed funding on the project at about the time of the experiment and other participants could not proceed with that work. Mr. Brett Delana has performed most of the analysis of the flight data.

IV Results of Data Analysis

A. General Status

The analysis is now essentially complete; final results will be reported in a paper now being prepared for submission to the Journal of Geophysical Research. Here we give only a brief summary of the key results. Statements made regarding the flight data are subject to review by other participants and therefore should not be considered final. However, the aircraft results are final.

B. Results from Aircraft Observations

During the early part of the portion of the flight when the accelerator was firing its programmed sequence, television systems on both aircraft in the conjugate region were oriented properly to detect artificial auroras if produced (see Fig. 2). None were detected, and from flight data we now know that probably none were produced. The one and only aurora seen was produced by Pulse B44 (last pulse in the second sequence). Prior to that pulse the program called for a sequence of 5 Kev electron bursts which might not have produced detectable auroras. Following Pulse B44 by 4 sec was Pulse C1 which was identical in current, voltage and duration. Even though at least one TV was oriented properly to detect an aurora from this pulse, no aurora was detected. The aurora resulting from Pulse B44 was clearly identified on the TV recordings of two independent systems operated on one aircraft. These recordings are the only optical data available. However detailed analysis has yielded a number of interesting results.

By a reiterative process involving testing of various models of the geomagnetic field and then employing the knowledge of the field line orientation obtained from a suitable field model it was possible to determine the position in space of the artificial aurora. The result is unique but less precise than would be provided by triangulation had observations from both aircraft been available. The method requires the assumption that the artificial aurora is field aligned, and the accuracy is somewhat dependent upon how well the field model finally chosen actually describes the orientation of the magnetic field. Three field models, POGO 8/69 epoch 1964.3, POGO 10/68 epoch 1965.8 and OGO 246 epoch 1965.3 were found to be satisfactory. These three models all predicted the actual areal location of the aurora to within 3 km and were in close agreement when used to determine the altitudes of the top and bottom of the aurora. These altitudes were 116 ± 2km and 92 ± 2km respectively. The altitude of maximum brightness was 102.5 ± 2km. These values are in satisfactory agreement with theory, the voltage of the electron pulse being 24 Kev.

A major result of this experiment was that an artifical aurora was observed in the hemisphere conjugate to the accelerator. That observation alone proves that it is possible to propagate a substantial beam of electrons for great distances along magnetic field lines, the distance in this case being approximately 7000 km.

Another major result comes from the high precision of the technique of tracing out magnetic field lines. Shaped charge barium tracer experiments conducted by us and LASL a year prior to this experiment demonstrated that no existing field model updated to the epoch of the tracer experiments accurately defines the field configuration at this location - an L = 1.27 field line terminating near Hawaii. The electron accelerator experiment verifies and improves upon the earlier results. Note from Fig. 3 that several tested field models are substantially in error at this location and that the three satisfactory models agreed with the observations only when updated to epochs near 1965, seven years before the experiment.

No accurate measurement of the auroral brightness was available however it was estimated that the artificial aurora produced an image on the TV screen roughly equivalent to that of an IBC II aurora. If viewed parallel to the magnetic field instead of 33° off-field the brightness would have been approximately 35 times greater or about 3.5 times as bright as an IBC III aurora. Such an aurora represents an energy deposition of approximately 2 ergs cm^{-2} sec^{-1}. From this value and the observed diameter of the artificial aurora, the required energy deposition would have been $6 \pm 3 \times 10^{10}$ erg sec^{-1}. The responsible electron pulse had current 160 ma and voltage 24 Kev and so approximately 4×10^{10} erg sec^{-1} was contained in the pulse. Whereas this value is quite accurate, the estimate of observed energy deposition is only that, an estimate.

However comparison of the ejected energy and that calculated from the observed auroral brightness indicates that there was no substantial in-transit degradation of the beam. Therefore it appears that instabilities or other loss processes as the beam traveled through the ambient magnetosphere environment were unimportant.

The artificial aurora was detected in the conjugate region at 15:06:22.06 ± 0.025 sec and the beam was initiated at 15:06:21.86 ± 0.00 sec. Assuming no unknown clock errors on the aircraft or at the Kauai range, the travel time was 0.20 ± 0.025 sec. The theroetical travel time for 24 Kev electrons is near 0.08 sec, so there may be clock or other error.

Two methods have been employed to determine the height luminosity profile of the artificial auroral ray. One method, unsatisfactory because of extreme scatter in the results, involved electronic sampling of the original video tape signal using a video analyzer. The second method utilized photography of a TV screen to produce a negative, which was then scanned with a densitometer. The light intensity is related to film density by $(d/10\gamma) \alpha I$, where d is the density, I the intensity and γ is the slope of the curve of density versus log exposure. Gamma(γ) is a function of the film, film exposure and development, TV camera electronics and TV screen characteristics. No direct calibration of these factors affecting γ were made. However tests of the TV system have shown that $\gamma \sim 1$ for that system. Film used was from one Kodak batch number; it was developed all at one time to ensure uniformity and $\gamma=1$ as nearly as possible. Calibrated step wedges were exposed on the film together

with the TV data. In subsequent calculations an overall system $\gamma=1$ was assumed. The effect of $\gamma<1$ is to sharpen the peak of the resulting height-luminosity profile; $\gamma>1$ flattens the peak. However such errors would not change the altitude of peak intensity or alter the basic shape of the curve. Results are given in Fig. 4, where a 3-point running average of sampled points is plotted. In Figure 4, height-luminosity profiles obtained each 0.1 sec of the 1-sec auroral ray lifetime are given. Figure 5 contains a plot of the altitude of peak intensity versus time and Figure 6 presents a plot of peak intensity versus time. These plots show a tendency for the altitude to increase with time during the last part of the aurora and for an increase in intensity during the first 0.3 sec. The later increase is probably due to increase of OI 5577 emission with time, owing to the 0.7 sec lifetime of the parent excited state. The increase of altitude with time could be due to similar reasons or due to minor velocity dispersion in the propagating electron beam.

In the process of the height-luminosity profile computations, the diameter of the auroral ray was found to be 210 ± 500 m. In arriving at this value the inherent widening of the streak by the observing instrumentation was taken into account. The resulting diameter is roughly twice the diameter of artificial auroras obtained earlier in a downward injection of electrons (130 ± 50 m).

The height luminosity profiles in Figure 4 do not resemble those of natural auroras, which generally show a sharper cutoff below the peak and greater luminosity at altitudes higher than the peak. To

verify that the artificial aurora profiles were not a consequence of the analysis method we used the same procedure on TV data taken on a natural aurora of comparable brightness and viewing aspect. Figure 7 shows data sets from artificial and natural aurora normalized to coalessce at the peak. The curves are similar below the peak but the natural aurora has greater relative intensity above the peak. Such differences are expected because the artificial aurora is produced by nearly monoenergetic electrons and most natural auroras result from an energy distribution with high fluxes at lower energies.

Following Berger et al., 1970, Wilmot Hess calculated altitude profiles of $A[Z_m(\ell)] \cdot D(h)$ for several electron energies taking into account the magnetic dip angle and atmosphere at the location of the artificial aurora. $A[Z_m(\ell)]$ is a penetration factor and $D(h)$ is the atmospheric density. The result, given in Figure 8, is indicative of an actual beam energy near 18 Kev instead of 24 Kev. However, the altitude of the peak is critical dependent upon the employed model of atmospheric density, and it is known that the density at these altitudes is quite variable.

C. Results from Flight Data

Operating instrumentation aboard the accelerator included three chaneltron electron detectors, three retarding potential analyzers, a two-axis altitude magnetometer, gyro controlled attitude control system and monitors of various functions such as accelerator current and voltage and monitors to measure current from the 4 sectors of the 22-meter diameter neutralization screen.

1. Payload Trajectory

Redundant radar systems at the Kauai Test Range yielded consistent tracking data, and it is thought that the trajectory obtained from the radar data is precise to within a few hundreds of meters and probably to within a few tens of meters. The trajectory was along azimuth 209° with apogee at 398 km achieved 150 km downrange. Figure 9 shows a plot of accelerator altitude versus time in the flight.

2. Payload Attitude

Payload attitude was maintained by gas jets controlled by a gyro-stabilized inertial platform. The inertial platform was so designed to operate only when the payload axis (the direction the accelerator pointed) was within 20° of the attitude at launch (45° between launch attitude and the direction of the local magnetic field) Following separation of the payload at T + 105 sec, the payload was despun (T + 107 sec) and the attitude control system was initiated (at T + 116 sec). Figure 10 contains a plot payload attitude relative to the launch attitude during the first 210 sec of the flight as determined by telemetered output of the gyro platform. The plot shows a drift away from the launch altitude of 11° during the first 105 sec. After separation and despin, the output indicates that the payload was brought back to near the launch attitude during the next 20 sec. According to the gyro data the attitude underwent a 10° excursion and returned to near launch attitude between T + 130 sec and T + 145 sec. The collector screen was deployed at T + 144 sec, and at T + 148 sec the attitude control system was shut down. Starting near T + 160 sec, the payload underwent a violent maneuver that caused the gyro platform to fall

outside its operating range. From T + 172 sec to T + 207 sec the gyro data indicate that the payload axis was inclined by more than 20° from the attitude at launch. If the attitude of the payload was along the magnetic field at the time of ACS shutdown (T + 148 sec), then the payload pitch angle values shown on Fig. 10 and subsequent diagrams are in error by 40°. Figure 2 shows the payload attitude relative the $\vec{B}$ throughout the flight.

3. Accelerator Performance

The accelerator was first pulsed on, as planned, at T + 192 sec, at which time the payload altitude was 300 km. During the first 20 pulses of the first (A) sequence, monitors of beam voltage and beam current showed erratic behavior. Programmed beam voltage was achieved only when the beam current was zero, and programmed beam current was achieved only when the monitor of anode current recorded currents greater than 250 ma, whereas the monitor of collector current recorded only minimal current being collected from the ambient plasma.

Beam voltage was nominal during the next 34 pulses (to pulse B 10) but the beam anode and collector currents were all zero. The anode current remained zero thereafter i.e., through pulse E9. The beam current rose slowly over the span of the 20 pulses following pulse B 10. Following pulse B10, the collector current was approximately equal to the beam current during each pulse. However, the beam current achieved was only approximately 30% of the programmed value during the remainder of the accelerator operation; the maximum current being 156 mamp. Pulse B44, the only pulse producing a

detectable aurora, was the first pulse achieving the maximum beam and collector current. On the basis of the current and voltage monitors there is no explanation of why pulse B44 produced a detectable aurora whereas similar subsequent pulses did not. Following pulse B44, televisions on the aircraft in the conjugate region were pointed properly to detect auroras if produced somewhat less than half the time.

We interpret the behavior of the beam voltage and the beam, anode and collector currents as indicating that substantial arcing occurred in one or more of the accelerator's six electron guns during the early part of the flight. Arcing evidently continued during the first 20 pulses and caused cathode poisoning of all six guns. It is possible that malfunction of an altitude thrustor may have emitted unwanted gas to cause voltage breakdown in the guns.

After pulse A20, arcing apparently ceased, and the damaged cathodes began to recover by burning off of the cathode poisoning to expose fresh cathode material. The partial recovery to roughly one-third of the nominal performance suggests that only two guns or their equivalent recovered. Since the collector current ran in unison with beam current after the initial erratic behavior of the accelerator, we conclude that the collector screen was able to maintain payload neutrality.

4. Results of Analysis of RPA Data

The flight payload contained three retarding potential analyzers having sensitive geometries of 13.1 cm^2 and acceptance angle 1.57 steradians. These were furnished by E. R. Maier of Goddard. One RPA was mounted on the accelerator gun deck with its sensitive trap normal in alignment with the accelerator beam axis and pointing forward. Two RPAs were mounted on the aft bulkhead so as to view directly opposite the forward RPA. The retarding voltage on the forward trap and on one rear trap was swept from -500 volts to -2 volts in 100 msec. The retarding voltage on the other aft trap was alternately switched between -3 volts and -8 volts at 2 sec intervals. Analyses of the RPA data undertaken so far have been aimed at learning the general characteristics of the data throughout the flight and at trying to understand the differences if any between the pulse creating an observed aurora and other pulses.

Examination of the data from the front RPA showed that the data acquired during accelerator pulses could be categorized into three classifications according to the recorded energy spectra. Most (69%) spectra indicated a moderate flux of particles of energy greater than 500 ev. Twenty-four percent of the pulse intervals showed a spectrum composed of a relatively weak flux of the > 500 ev component and a moderate flux of supra-thermal particles in the energy range 2-100 ev. The remaining 7% of the spectra indicated only the presence of the 2-100 ev supra-thermal component. This

low energy spectral type was observed only during the 34 pulse interval following pulse A20 when the accelerator was recovering from the initial erratic behavior. Once the accelerator beam current exceeded 100 mamp, the RPA spectra were of the high only or mixed high energy-suprathermal types. Whenever the high energy flux appeared, its onset was without observable delay at the times of accelerator firing. The total net flux intercepted by the front RPA was consistently much higher (sometimes by a factor of ten) during the pulses of high energy and spectral type than for those of the mixed high energy-suprathermal types. Figure 11 shows the fluxes of the high energy component during the latter part of the flight.

The shape of the RPA spectra appeared to be unrelated to the accelerator beam voltage. Statistically the maximum appearance of the mixed high energy-suprathermal spectra occurred at accelerator pitch angles near 105°-110°, as determined by the onboard magnetometers, but a clear, detailed dependence upon pitch angle is not evident see figures 12 and 13. During pulse B44, the one producing a visible aurora, the front RPA spectrum was of the high energy type with moderate flux level. The flux level was approximately 80% higher on the next five pulses; the spectral shape remained unaltered.

Energy spectra observed with the rear sweep RPA were of the same types as those observed on the front (sweeping) RPA, and, in addition, 14% of the spectra showed zero flux. Thirty-nine percent of the spectra showed a small to moderate flux of suprathermal electrons only; 27% showed only greater than 500 ev flux and 21% showed the mixed high energy-suprathermal energy flux. The >500 ev flux

spectral type occurred mainly in the payload pitch angle range 100°-120°; the low energy components predominated at payload pitch angle ranges 60°-80° and 120°-140°, and the zero flux spectra were concentrated near pitch angles 40°-60° and 155°-180°. Flux levels observed by the rear sweep RPA were quite variable. The fluxes observed during the five pulses following B44 were two to three orders of magnitude lower than for pulse B44. Acting as essentially a measurement of total flux, data from the rear fixed RPA varied extensively during the flight without sensible correlation with payload pitch angle. The large total flux recorded during pulse B44 was exceeded during only three other pulses; during those pulses any auroras produced were unobservable. Following accelerator turnoff at the end of certain pulses there were persistent suprathermal fluxes lasting up to 250 msec. On several occasions these were seen simultaneously on the front sweeping RPA and the rear fixed RPA but they were most frequent on the rear RPA. Such persistent fluxes were almost always associated with pulses having the mixed >500 ev - suprathermal spectra. These fluxes lasted longest during the early part of the flight when the payload velocity transverse to the magnetic field was lowest. Relating the persistent time and the payload transverse velocity yields the result that the average diameter of the region where persistent suprathermal fluxes existed was 80-100 m; in some cases the diameter was as large as 200 m. The observed diameter following pulse B44 was 96 m, roughly half the diameter of the related aurora in the conjugate region.

5. Results of Analyses of Energetic Particle Data

Little data of value seems to have resulted from the three channeltron detectors placed facing forward on the accelerator deck. Two detectors were shielded with 45 micrograms cm^{-2} Al so as to detect only > 6 kev particles and one shielded with 100 micrograms cm^{-2} Al to be sensitive to >13Kev electrons. The >6Kev detectors were saturated throughout the flight. Output from the >13Kev detector was scaled to determine the ambient flux in the fraction of a sec just prior to each pulse. The resulting plot is shown as Figure 14. The results are extremely variable showing a rapid increase from the threshhold (a few counts per 3 msec sampling interval) to 380 counts per 3 msec as the payload rose through the 310 km altitude level. Thereafter, the flux dropped erratically to near threshhold values as the payload climbed to altitude 390 km. Starting with the B pulse sequence, the > 13 kev flux rose and fluctuated between 10 and 80 counts per sample. Following pulse B27 when the payload was near apogee, the detector went into saturation. Saturation occurs at fluxes somewhat greater than 500 counts per sample. The detector came out of saturation after pulse B39 and thereafter recorded between 8 and 512 counts per sample (average near 80) during the remainder of the flight.

Behavior of this detector during selected pulses is shown in Figure 15. There it is seen that the detector output typically goes to maximum at the initiation of an accelerator pulse. On Figure 15 the pulse is initiated at time -1.0 sec except for pulses labeled B18 and B42 where it is at a time just before -1.0sec.

Other exceptions are pulses B14, C18 and D18 where the pulse initiation is at 0.0 sec. As is characteristic of such a counter, the detector output falls from the maximum to the zero level in deep saturation. Typically, as is shown on Figure 15, the output goes to maximum as the accelerator is turned off and then shows decay thereafter. The detector outputs (in telemetry voltage) shown in Figure 15 are selected mainly because each shows some irregularity in the decay after the end of each pulse.

The dashed lines on Figure 15 indicate the time measured from the end of each pulse for 20 Kev particles to travel to the the conjugate atmosphere, be scattered, and to travel back to the payload. The dotted line similarly shows the time of travel for mirrored particles. The letter x placed after each pulse shows the time from required for the payload to travel 100 m transverse to the magnetic field, i.e. to reach the edge of a return beam 200 m in diameter. If the x lies to the left of the dashed and dotted lines there would seem to be no possibility that the detector would intercept a return beam from the conjugate hemisphere. It seems unlikely that any characteristics of the detector output can be taken to imply detection of a returned beam. Unfortunately, the detector was in saturation following pulse B44, the only pulse for which there is any assurance that a return beam existed, simply because an aurora was seen and some backscattering must have occurred.

6. Interpretation and Summary of Flight Data

Behavior of the beam voltage, beam current and anode current through pulse A20 indicate that substantial arcing occurred in at least one of the six electron guns and caused cathode poisoning of all. It is possible that an altitude thrustor malfunction caused this trouble. Recovery of the guns apparently occurred during the next 34 pulses as a consequence of burning off of the cathodes to expose fresh emissive material. During this interval the beam voltage was nominal but there was no beam, anode or collector currents and so there was no beam production or return neutralization current. After the guns stabilized, the accelerator operation appeared to be normal except that the actual beam and collector currents never rose to more than one-third the programmed values, and the voltage was 25% higher than expected. In this phase of the flight, collector current matched the beam current, indicating effective neutralization of the accelerator.

As yet, uncertainty remains about the payload attitude during the flight. We are still in hopes of removing apparent discrepancy between gyro and magnetometer attitude measurements. Nevertheless it does appear now that the payload tumbled throughout the flight with period 70 sec and that the accelerator was rarely if ever properly pointed parallel to the magnetic field.

The high energy (> 500ev) particles detected by the retarding potential analyzers probably were secondary electrons generated from primaries ejected by the accelerator. Since the rear

sweeping RPA saw >500 ev electrons less frequently than the front RPA, it appears that source of these particles was near the front of the payload. In this observed flux there was no indication of particles reflected from the conjugate hemisphere. Temporal variation in the >500 ev flux probably is related to payload altitude as there is no specific evidence indicating shielding by the collector screen. However, if the payload gyrated in the manner we think, it seems likely that the screen probably did not remain planar with its normal axis parallel to the accelerator axis.

Flux measurements taken with the rear fixed RPA hold a possible key to the question of why auroras were not observed with pulses other than B44. Only 3 of the 92 pulses subsequent to pulse B44 produced fluxes in the suprathermal range (2-500 ev) comparable to that of pulse B44. These three pulses, D3, D24, and D40 occurred when the airborne TV sytems were not pointed so as to detect any auroras produced.

In general, persistence of the 2-500 ev flux continued after pulse B13 and all subsequent pulses. The duration of these suggests that the accelerator primaries generated a ~~recording~~ secondary beam of diameter near 100 m. That the primaries did leave the accelerator is ~~implified~~ implied by the matching of collector and beam currents.

The results cited here are still under study. It is intended that a journal paper reporting the final results will be prepared in collaboration with other experiment participants.

REFERENCES

Davis, T. N., T. J. Hallinan, G. D. Mead, M. C. Trichel and W. N. Hess, J. Geophys. Res., 76, 6082, 1971.

Hess, W. N., Electron beam field mapping, NASA Goddard X-Doc. X-640-65-492, 1965.

Hess, W. N., M. C. Trichel, T. N. Davis, W. C. Beggs, G. E. Kraft, E. Stassinopoulos and E. J. R. Maier, J. Geophys. Res., 76, 6067, 1971.

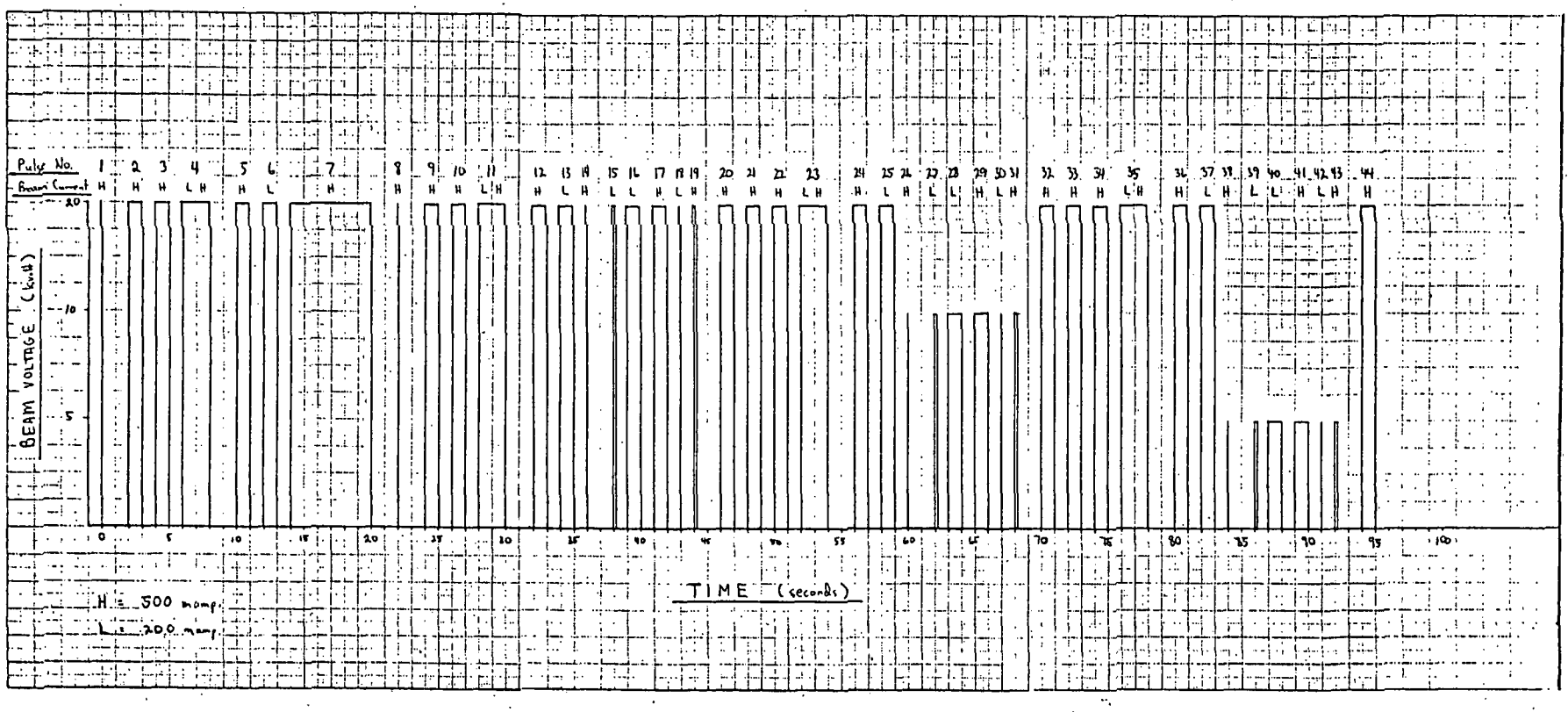

Figure 1. The nominal pulse program showing one sequence. A new sequence began upon the completion of that previous; herein the sequences are labeled in order A, B, C, D and E.

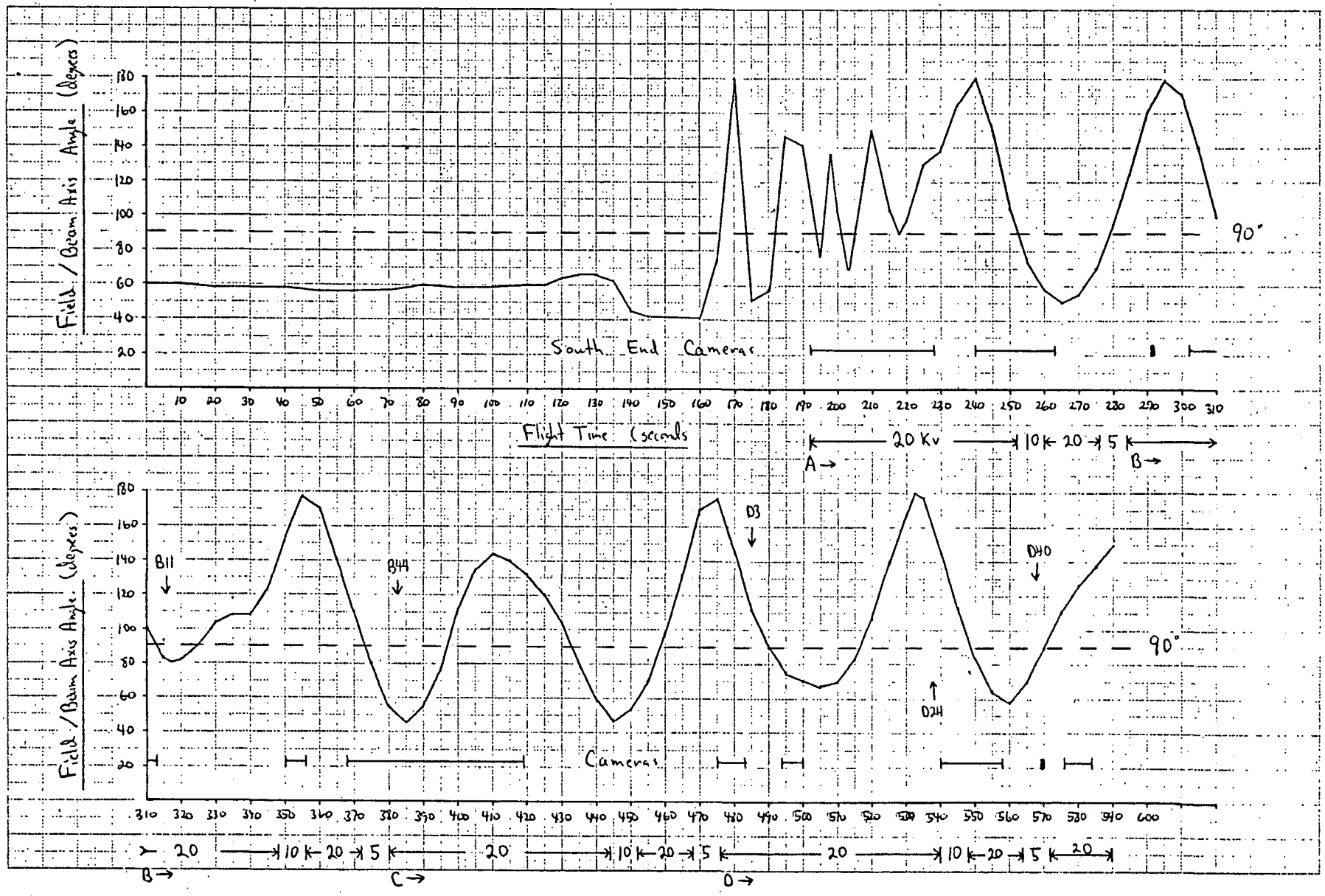

Figure 2 - Payload attitude determined from fluxgate magnetometers where 0° is upfield. Also shown are times of certain pulses, times when southern hemisphere cameras could detect auroras and the times of the various pulse sequences.

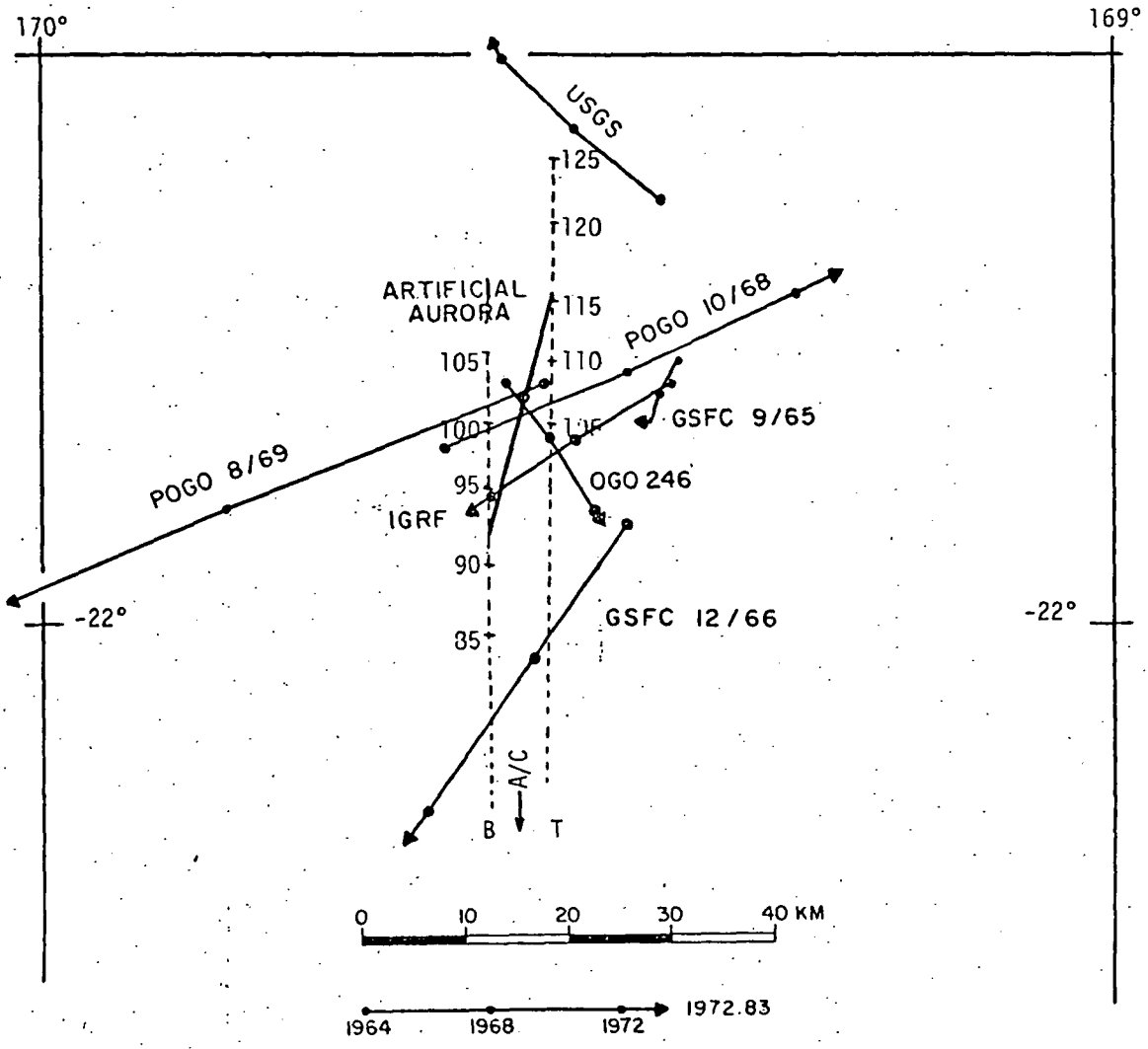

Figure 3 - Map showing the areal position of the payload conjugate point at 105 km altitude according to various field models updated as indicated at the bottom of the diagram. The heavy line shows the position of the artificial aurora; the open circle at its center is the 105-km altitude position. Dashed lines show the areal positions of the top (T) and bottom (B) of the streak as a function of altitude as seen from the observing aircraft.

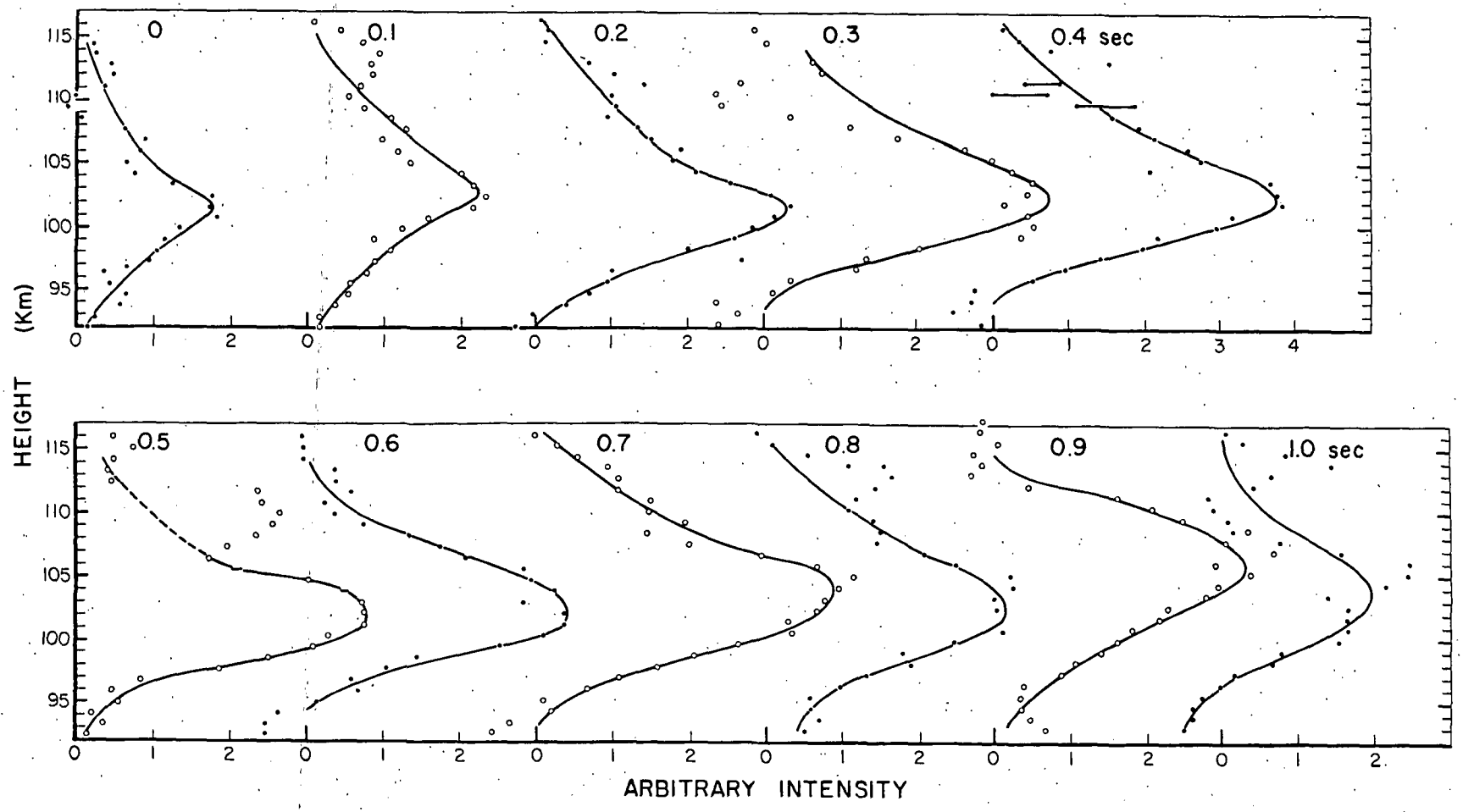

Figure 4 - Height-luminosity profiles obtained every 0.1 sec during the lifetime of the observed aurora resulting from Pulse B44.

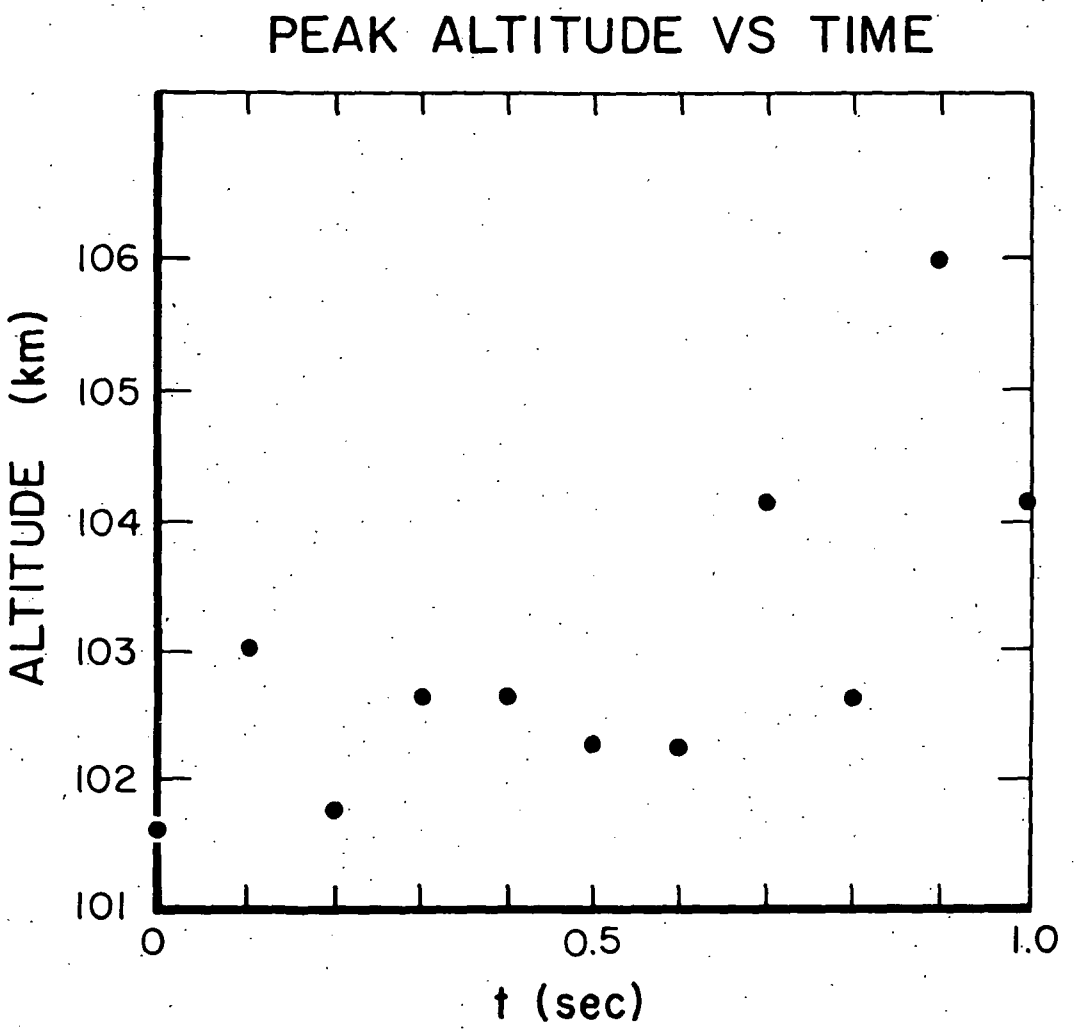

Figure 5 - Altitude of peak auroral intensity as a function of time during the observed aurora.

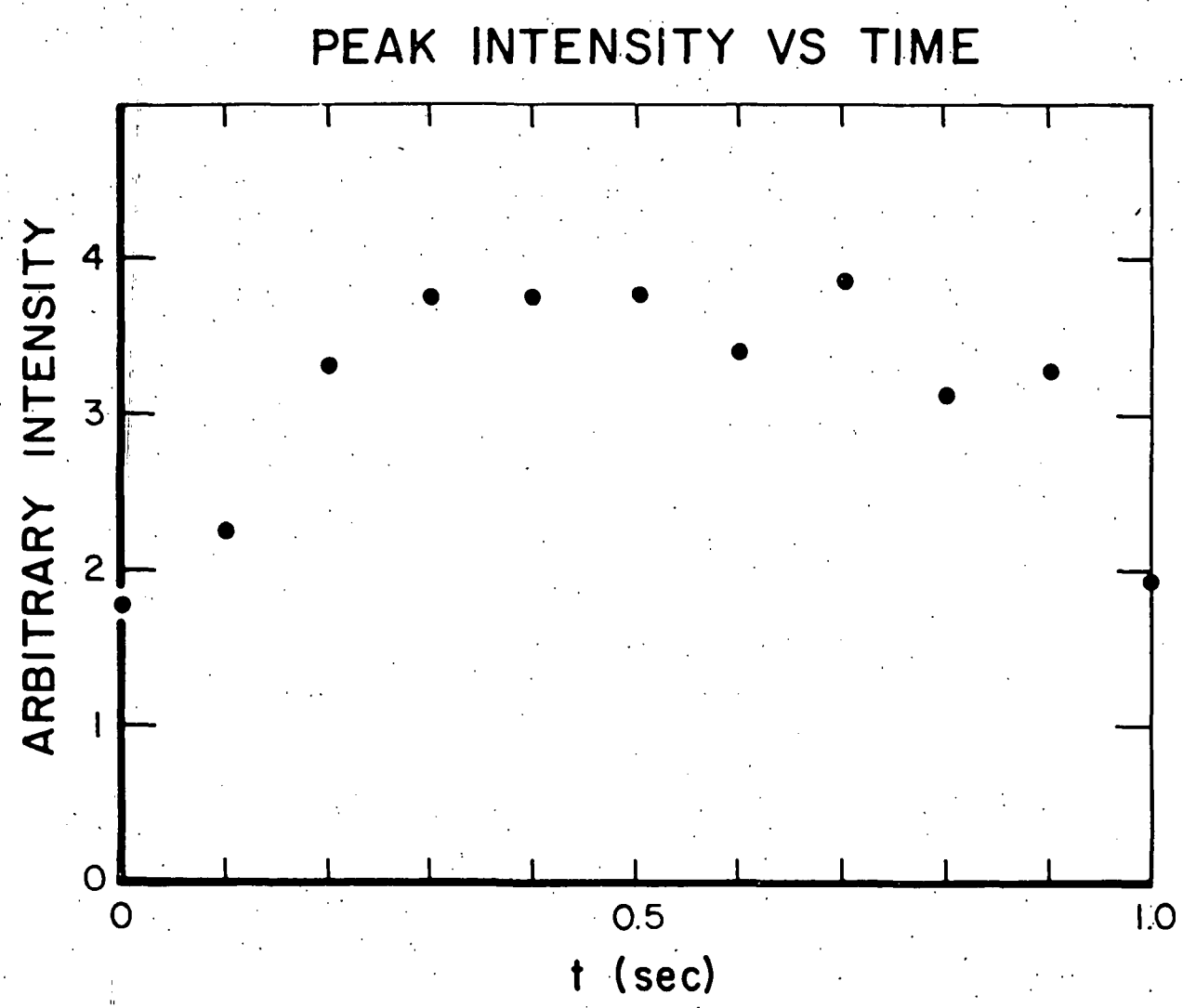

Figure 6 - Peak auroral intensity as a function of time during the observed aurora.

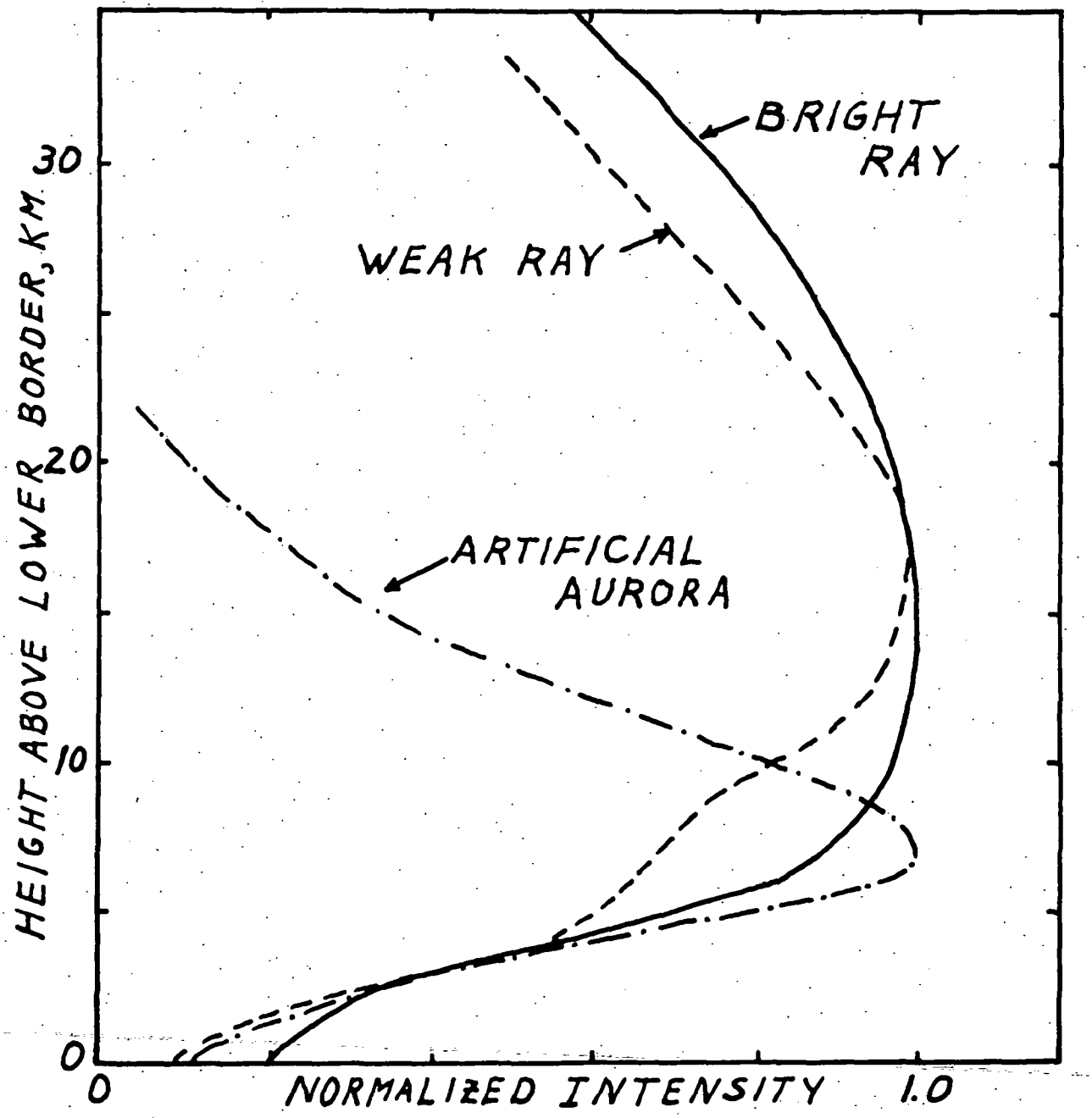

Figure 7 - Height-luminosity profile of the artificial aurora from pulse B99 and profiles of similarly appearing natural auroras measured by the same technique.

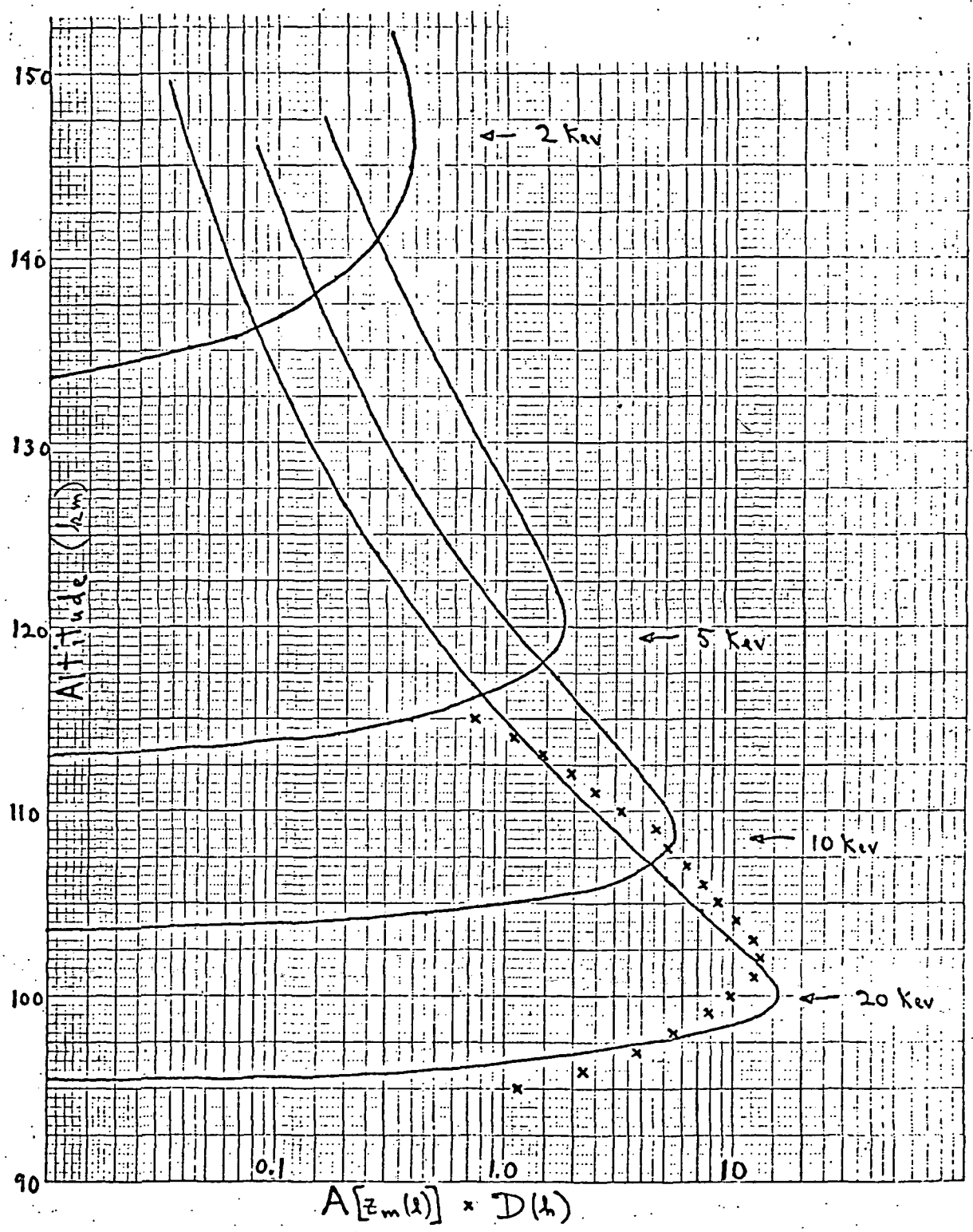

Figure 8 - Calculations by W.N. Hess of theoretical height-luminosity profiles (solid lines) compared to the observed profile (X) of the aurora from Pulse B44.

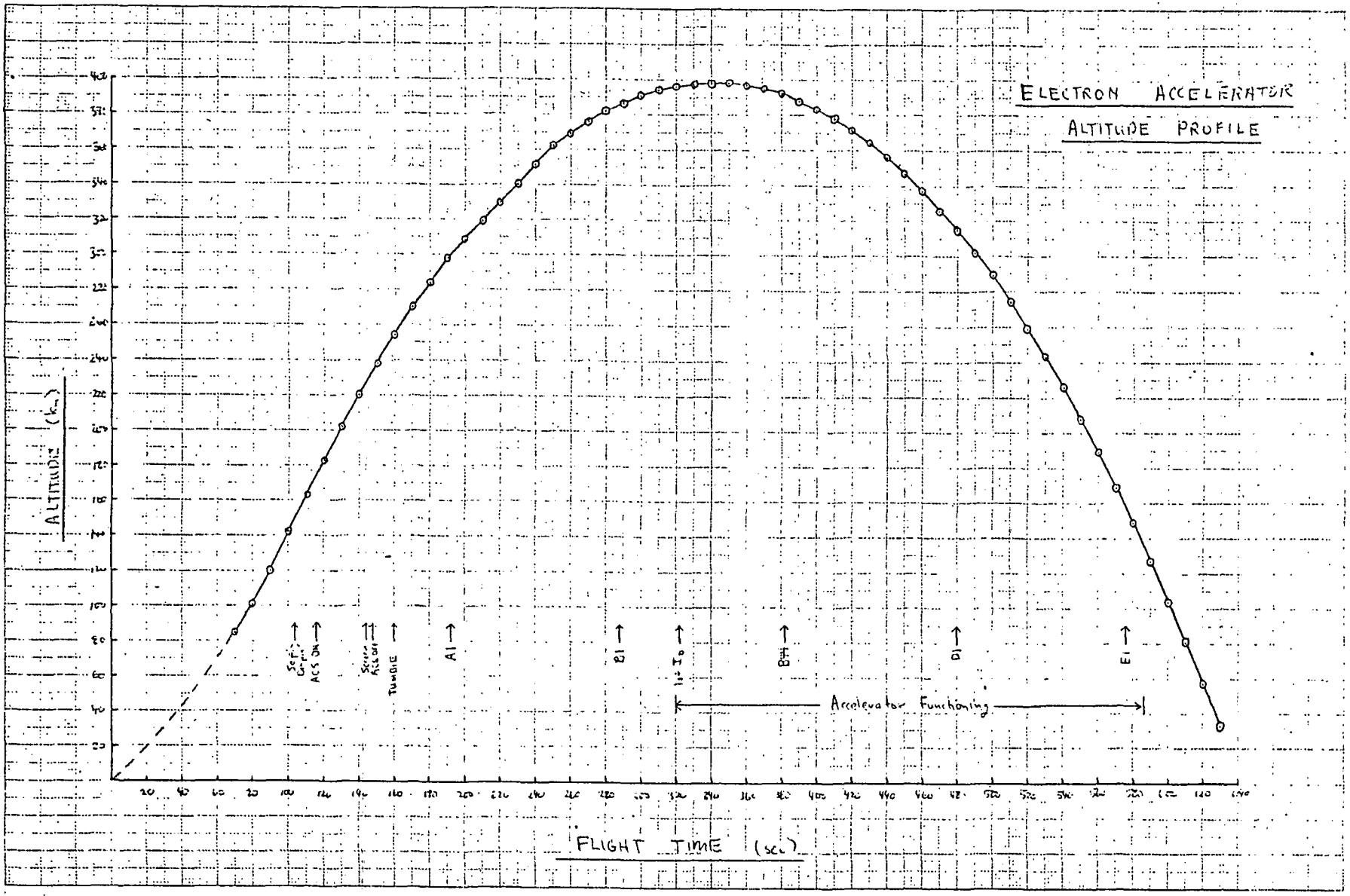

Figure 9 - Payload altitude versus time of flight.

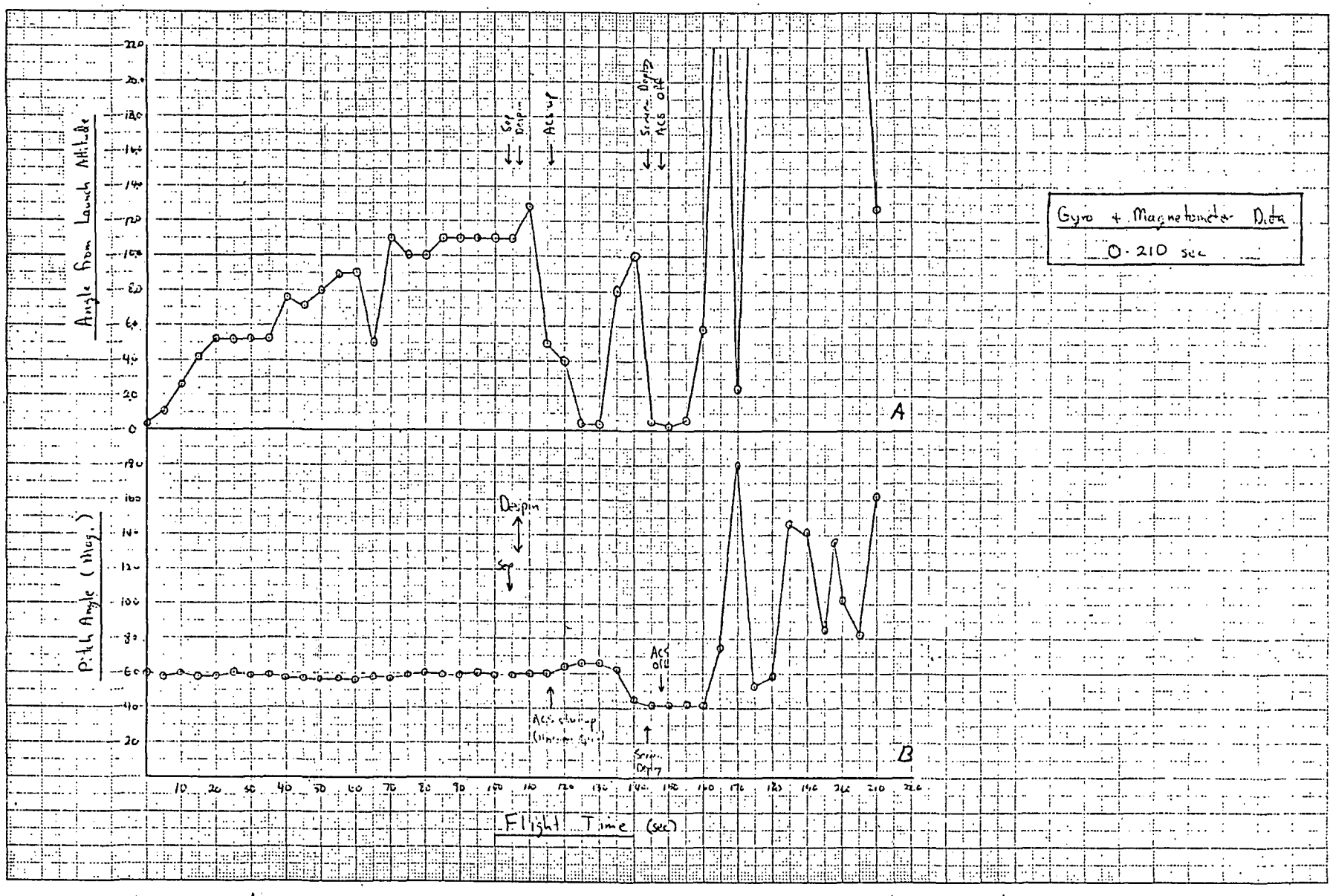

Figure 10 - Payload attitude during the early portion of the flight from gyro data (A) and from magnetometer data (B).

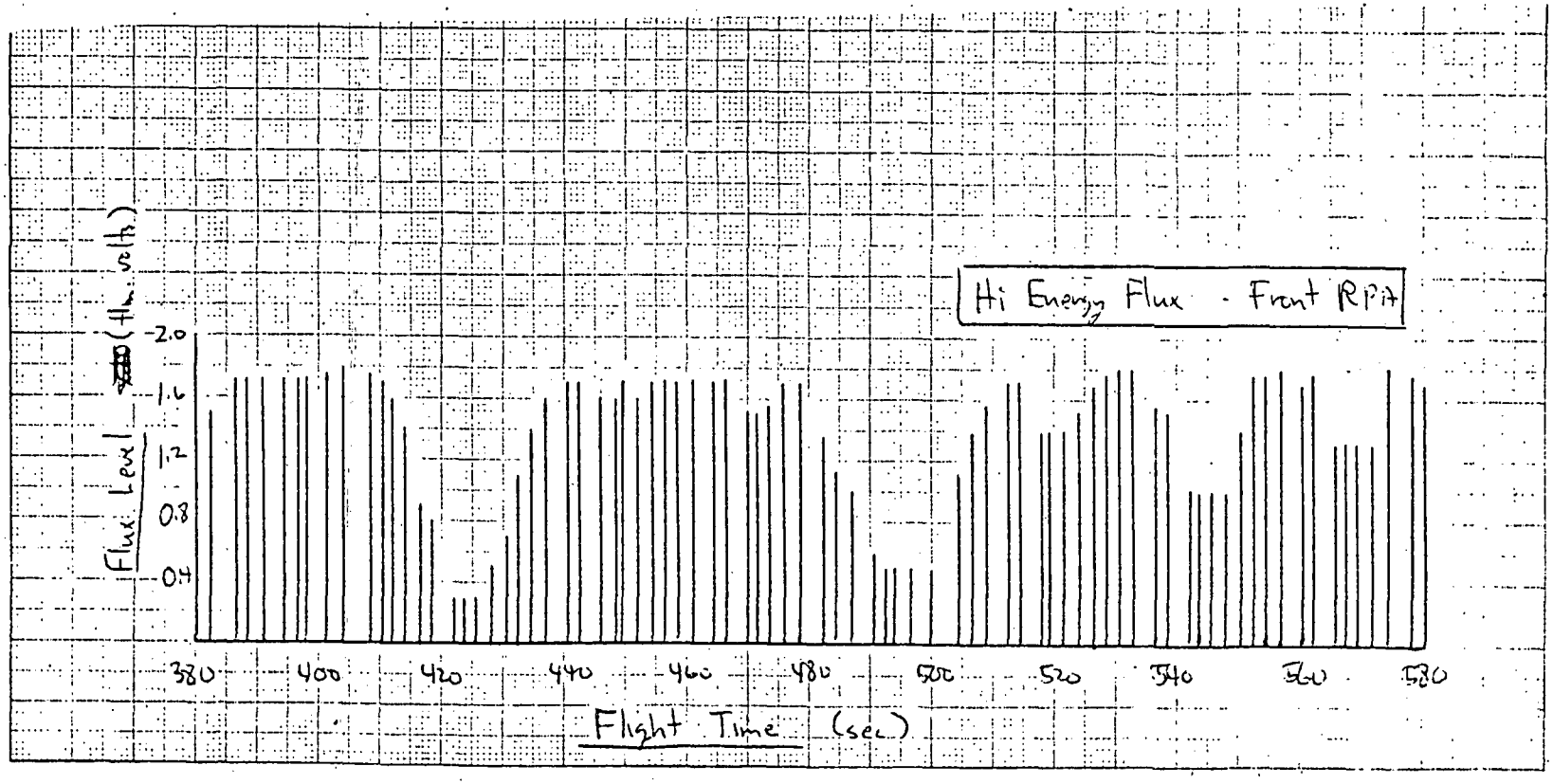

Figure 11 - Flux levels (in telemetry voltage) detected by the front RPA in the >500 ev component.

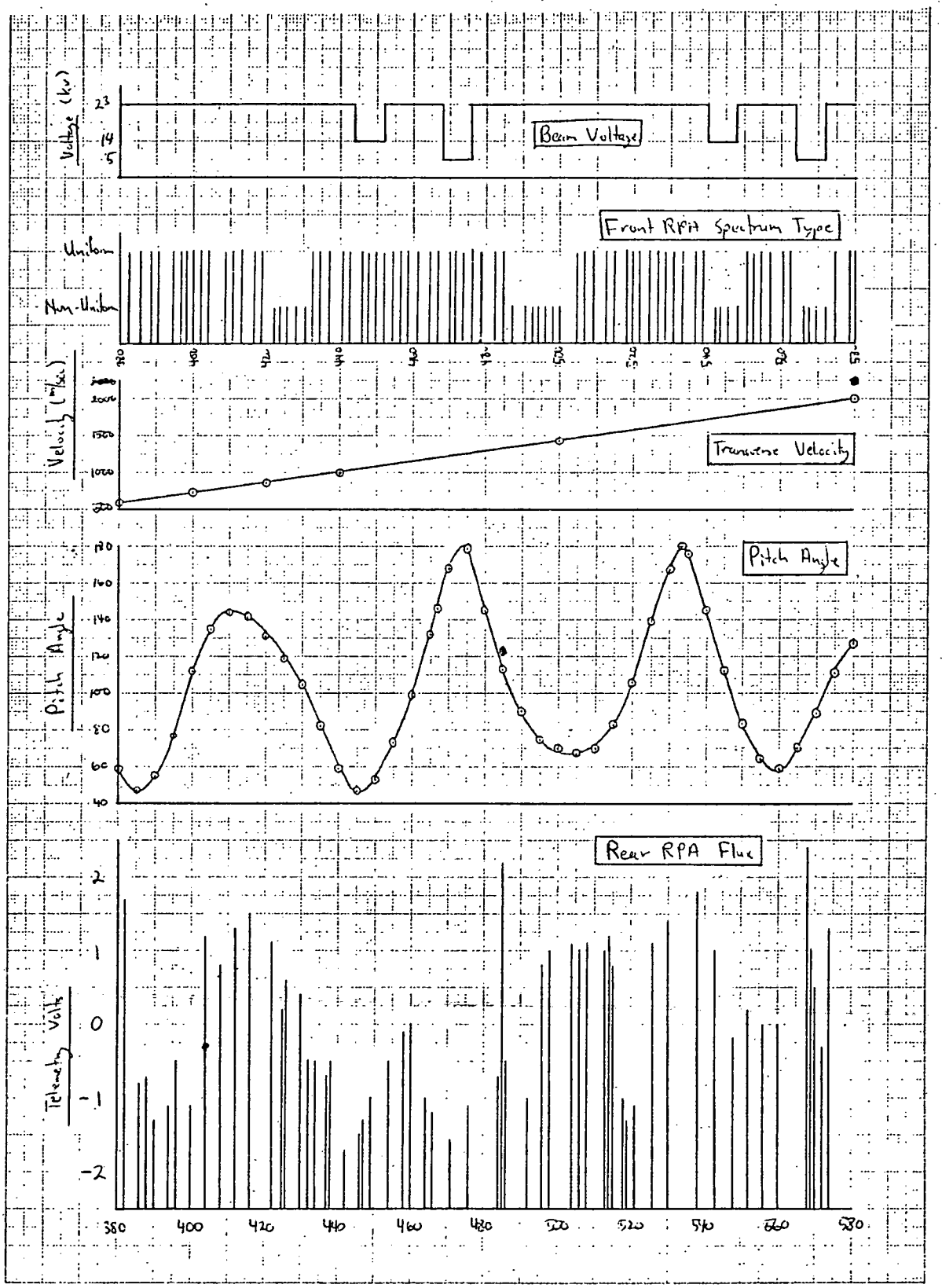

Figure 12 - Various parameters plotted as a function of flight time (in sec) during the latter part of the flight.

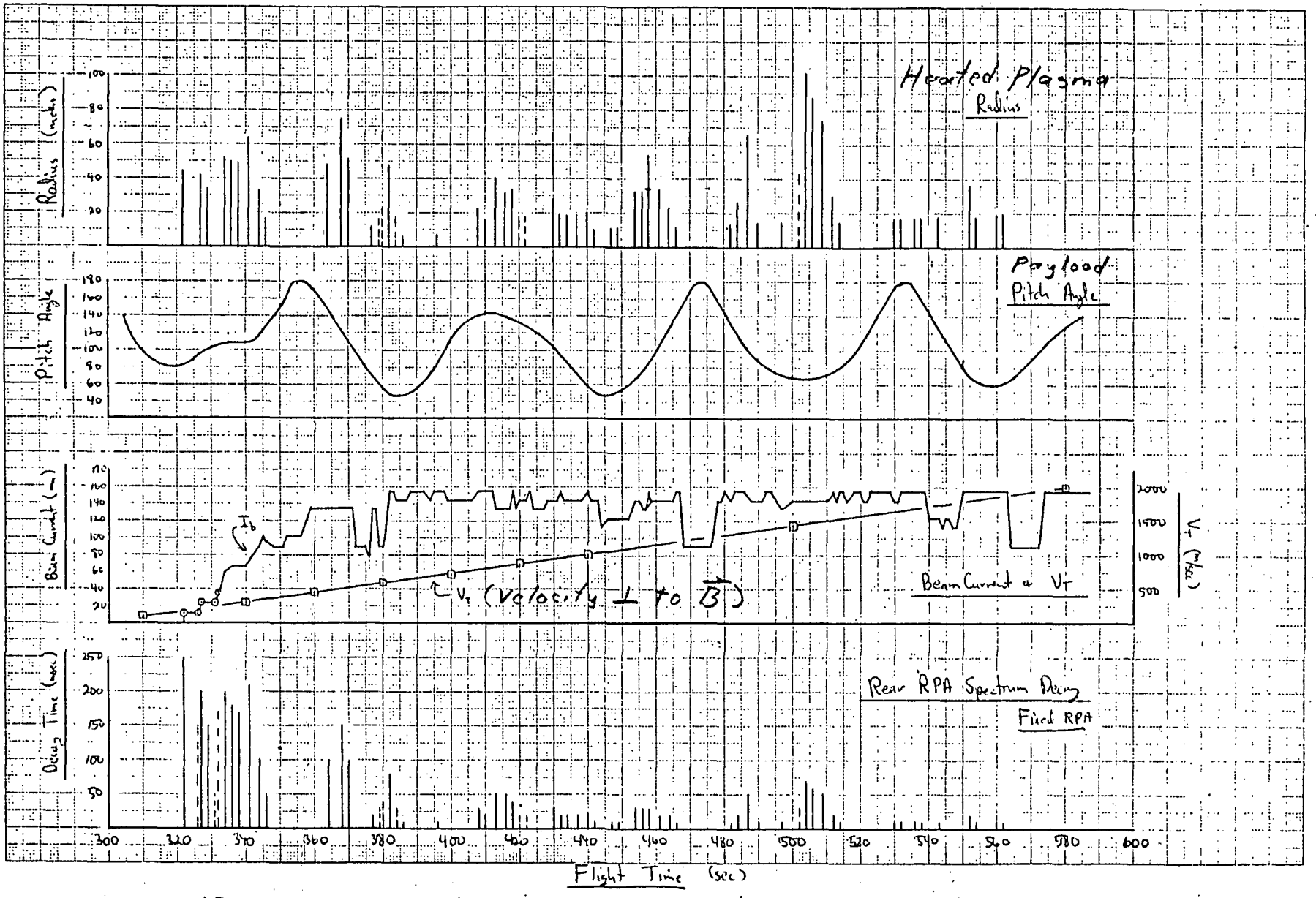

Figure 13 — Additional flight parameters or results, as in Figure 12.

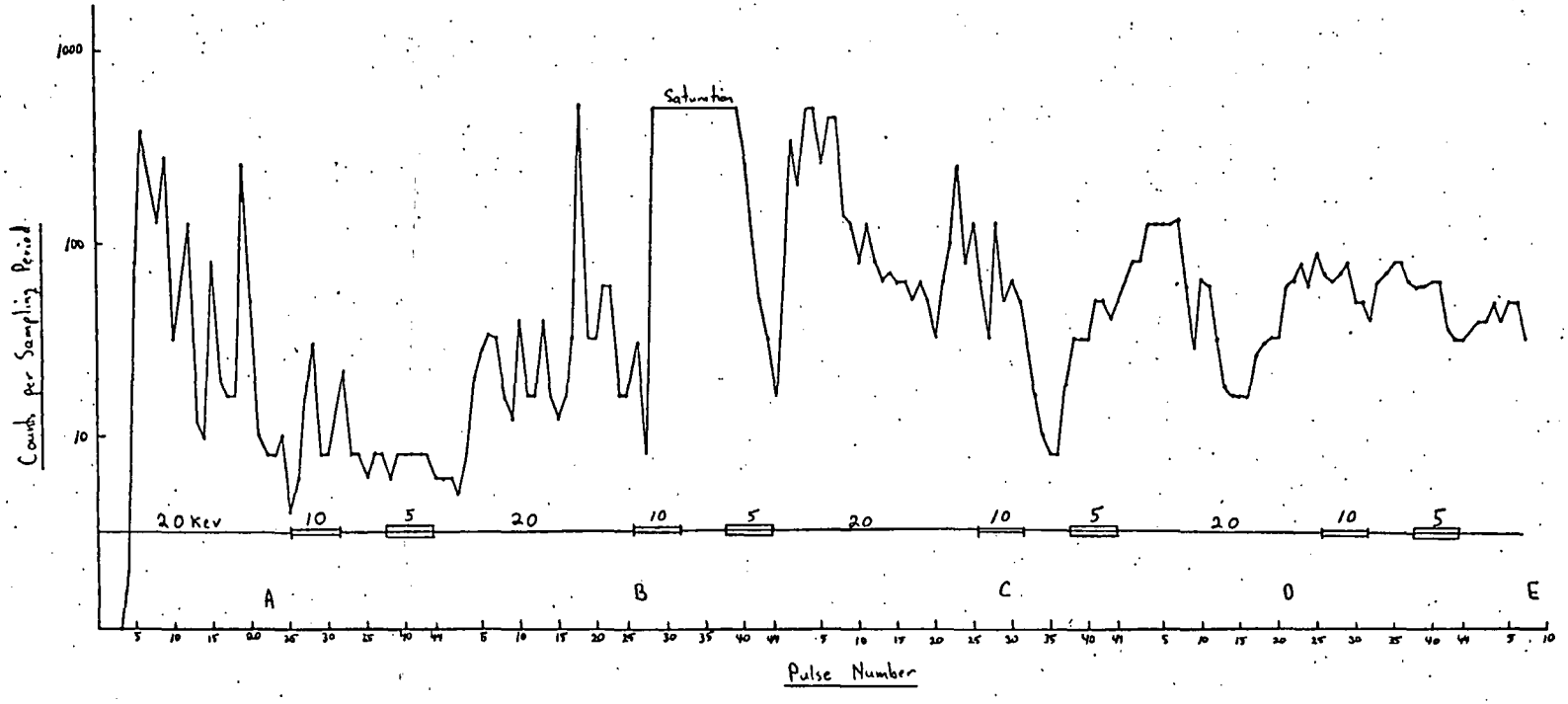

Figure 14 – Flux of >13 Kev electrons in counts per 3-millisec interval just prior to the onset of each accelerator pulse plotted as a function pulse number.

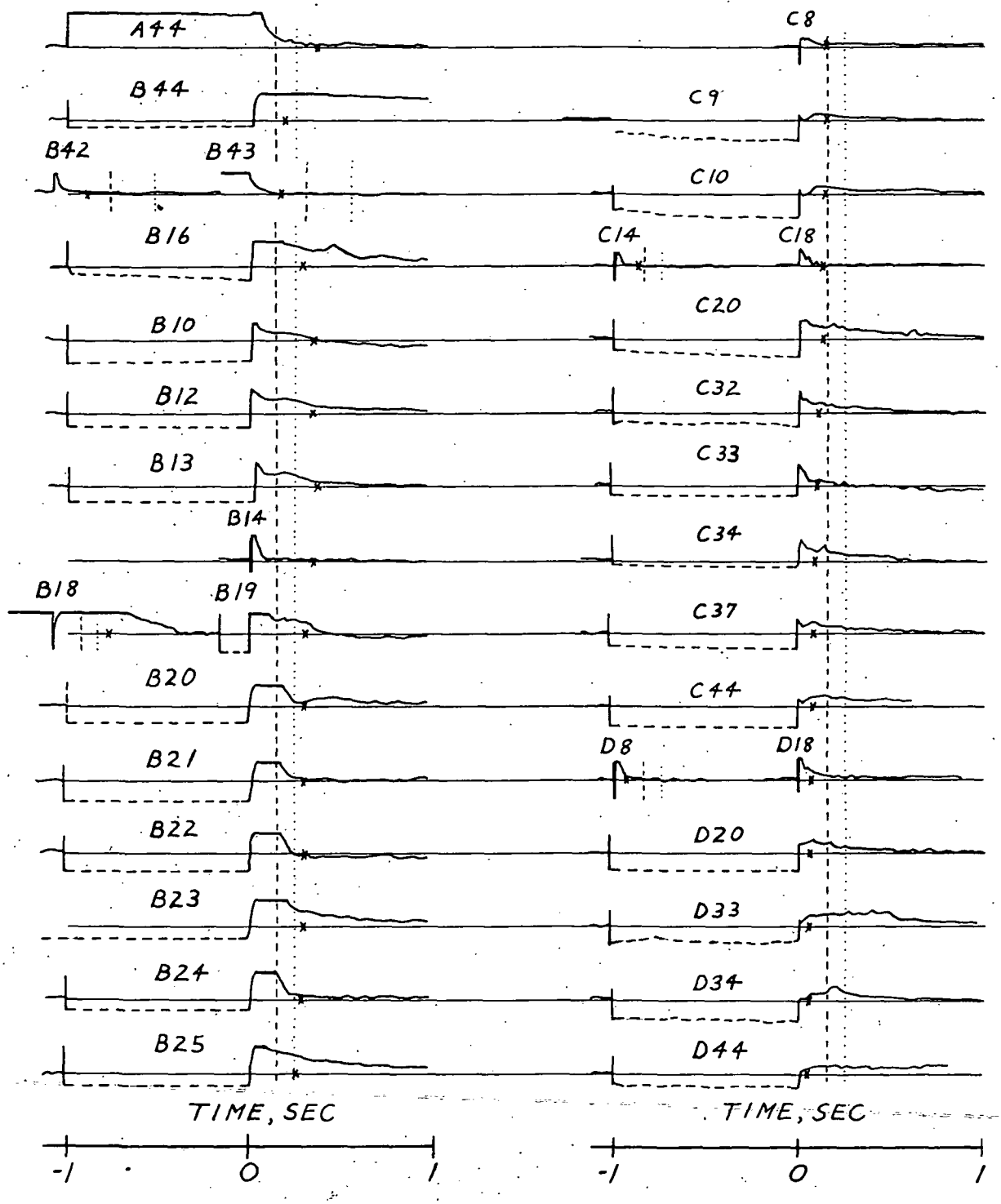

Figure 15 – Tracings of direct telemetry output of the >13 Mev electron detector near times of pulses shown. See text for explanation.